PROCEEDINGS, ATC-17-1 SEMINAR ON SEISMIC ISOLATION, PASSIVE ENERGY DISSIPATION, AND ACTIVE CONTROL, APPLIED TECHNOLOGY COUNCIL, SAN FRANCISCO, CALIFORNIA, MARCH (1993)

DESIGN- AND ULTIMATE-LEVEL EARTHQUAKE TESTS OF A 1/2.5-SCALE BASE-ISOLATED REINFORCED-CONCRETE BUILDING

Ian D. Aiken, Peter W. Clark, and James M. Kelly

Earthquake Engineering Research Center, University of California at Berkeley, USA

Masaru Kikuchi, Masaaki Saruta, and Kazuo Tamura

Shimizu Corporation, Tokyo, Japan

Abstract

This paper describes earthquake simulator tests of a 1/2.5-scale model of an existing base-isolated, three-story reinforced-concrete building in Japan. The building is one of a pair of buildings, one isolated and one fixed base, that were constructed to evaluate the effectiveness of seismic isolation. The earthquake simulator study consisted of four phases. In the first phase component tests of three different types of elastomeric isolation bearings were performed. Second, the building was tested on each isolation system in turn, to obtain direct comparisons of their performance. Two types of high-damping rubber isolators and one type of lead-rubber isolator were used in these tests, and bracing attached to the model to prevent damage to the concrete superstructure. In the third phase, the unbraced model was subjected to a wide range of earthquake inputs, this time with only one type of high-damping bearings. The most important tests in this phase were extreme earthquake inputs, sufficiently severe to cause substantial inelastic action in the superstructure and nonlinear stiffening behavior in the bearings. The final phase involved epoxy-injection repair of the concrete frame, and then moderate-level tests of the model in both isolated and fixed-base conditions. Results from the shake table tests show significant reductions in superstructure accelerations, interstory drifts, and base shear forces due to the isolation systems, when compared with the expected response of the equivalent fixed-base building.

Introduction

Twin full-scale buildings were constructed on the campus of Tohoku University in Sendai, Japan, by Shimizu Corporation for the purpose of evaluating and demonstrating the seismic performance of base-isolated structures (Yamahara and Izumi, 1987). The three-story, reinforced-concrete buildings are identical except at the foundation level; one has an ordinary fixed-base foundation while the other is base isolated (Figure 1). The structures are unoccupied, and both are fully instrumented to record earthquake ground motions and building responses. The foundation connections of the base-isolated building permit the isolation system to be easily changed, and since the completion of the buildings in 1986 four different isolation systems have been installed. These systems include natural rubber bearings and viscous dampers, high-damping elastomeric bearings, manufactured by both Japanese and U.S. companies, and most recently, a set of low-stiffness, high-damping rubber bearings from England. Each of the isolation systems has been kept in place for about 18 months, and the response of the various systems to a number of earthquakes has been recorded (Izumi et al., 1990, and Saruta et al., 1990). While there have been numerous earthquakes that have disturbed the twin buildings since their completion in 1986, none have been very large and the likelihood of a very severe earthquake hitting the buildings in the near future is not great. To obtain results that would

indicate the response of the full-size isolated building in a severe earthquake, an earthquake simulator study of a large-scale model of the building was undertaken.

A 1/2.5-scale model of the isolated building was constructed and tested on the earthquake simulator (shake table) at the Earthquake Engineering Research Center (EERC) of the University of California at Berkeley (Figure 2). The main objectives of the study were to fully identify the mechanical characteristics of three types of isolation bearings, to investigate the response of the large-scale model on each of the three systems under design-level motions, and to subject the isolated model to ultimate-level earthquake shaking, investigating the interaction between stiffening of the isolators and inelastic action in the concrete superstructure.

Description of Isolation Systems

Three types of isolation bearings were used in the earthquake simulator tests. Two of the bearing designs were reduced-scale versions of high-damping bearings that have been installed under the full-size building in Sendai, while the third bearing type was a lead-rubber design that has not been installed under the full-size building. The following sections provide brief descriptions of each of the bearing types, and a summary of the results of the tests of the individual bearings. A more detailed description of the component tests of the bearings is provided in (Aiken et al., 1992).

Design 1: High-Damping A

These bearings were made from a blend of filled natural rubber and a synthetic rubber. The compound is called KL301 by the manufacturer, Bridgestone Corporation, Ltd., Japan, and is one of a suite of high-damping elastomers that they have developed for seismic isolation applications. KL301 has a shear modulus of about 620 psi at very small strains, which decreases to 95 psi at 50 percent strain, 60 psi at 100 percent strain, and 50 psi at 150 percent strain. The design axial pressure was 470 psi. The bearings were designed with flange-type end plates to permit bolted structure and foundation connections.

Design 2: High-Damping B

These bearings were made from a low-modulus, filled natural rubber compound, designated HDNR-S by the developer, the Malaysian Rubber Producers' Research Association (MRPRA), England. The bearings were manufactured by Rubber Consultants, Ltd., England. The shear modulus of this material varies from about 115 psi at a shear strain of 5 percent to about 70 psi at 50 percent strain and 58 psi at 100 percent strain. The design axial pressure was 740 psi. Bearing-structure and foundation connections were bolted. Instead of using flange-type end plates, the bearings were connected by bolting directly into the top and bottom end plates.

Design 3: Lead-Rubber

These bearings were made from an unfilled natural rubber compound, and contained a 1-inch diameter lead plug. The bearings were manufactured by Oiles Industries, Ltd., Japan. For design purposes, the rubber shear modulus was assumed to have a constant value of 85 psi. The design axial pressure was 445 psi. These bearings had shear dowel end plate connections.

Component Tests of Isolators

All of the bearing tests were performed in a machine developed for general testing of small-to-moderate sized individual isolation bearings. Fifteen bearings of designs 1 and 2, and 12 bearings of design 3 were tested. The basic type of test performed on all the bearings was a sinusoidal horizontal displacement-controlled loading, conducted with either 11 kips or 17.6 kips constant axial load, for 5 cycles of loading at

shear strain amplitudes of 5, 25, 50, 75, and 100 percent. These axial loads were approximately those that the bearings carried under the model building on the shake table. The frequency of loading was 1 Hz for all of the basic tests. Other types of tests included cyclic shear tests at different frequencies and a range of different axial loads, large-strain cyclic tests, and monotonic shear and tension failure tests (Aiken et al., 1992). Some results from the basic tests and the shear failure tests follow.

Bearing effective stiffness and damping were calculated from the experimental results using the following relationships:

$$k_{eff} = \frac{F_{max} - F_{min}}{d_{max} - d_{min}}$$

$$\xi = \frac{W_d}{4\pi W_s}$$

where:

F_{max}, F_{min} = peak values of shear force

d_{max}, d_{min} = peak values of shear displacement

W_d = hysteresis loop area

$W_s = \frac{1}{2} F_{max} d_{max}$

These properties are plotted as a function of shear strain for each bearing type in Figure 4. The design 1 and 3 bearings show very similar effective stiffness-strain relationships. This is to be expected, as the original design intent for these two types of bearings was that their stiffness properties be the same. The design 2 bearings, however, show a much lower stiffness, about one-third of the stiffness of designs 1 and 3 over the entire strain range. The damping ratios of the three designs show greater differences.

Typical hysteresis loops for the three types of bearings under sinusoidal shear displacement loading are presented in Figure 3. The loops shown for the high-damping A bearing are at shear strains from 200 to 350 percent, for the high-damping B bearing from 100 to 250 percent, and for the lead-rubber bearing from 50 to 200 percent. Beyond a certain strain level the high-damping bearings exhibit a clear stiffening behavior. This stiffening is a material property of filled rubbers. The lead-rubber bearing, which was made from unfilled rubber and had doweled shear connections, did not show the large-strain stiffening effect.

The shear force-displacement relationship for a design 1 bearing loaded to the point of shear failure is shown in Figure 8. The high-strain stiffening behavior is clearly seen. Beyond a strain of about 250 percent the bearing stiffens appreciably, and at the point of failure (739 percent strain) the force in the bearing is about 6 times that at 250 percent strain. This result indicates an enormous reserve strength beyond the design level.

Test Model

The test structure was designed and constructed to be a 1/2.5-scale model of an existing three-story, reinforced-concrete base-isolated building. Member stiffnesses and yield strengths were carefully scaled, and the concrete mix designed to match the strength of the concrete in the fully-size building as accurately as possible. The model had a total weight of 90 kips, with uniform floor weights, uniform interstory heights

of 47 inches, and stood approximately 180 inches in height above the shake table platform (Figure 2). The model was isolated on six bearings, and foundation details permitted the bearings to be easily changed. A total of 156 model and shake table response quantities were measured in each test. Accelerations and displacements were measured at each floor level, and rebar strains measured at each beam-column joint interface in one frame of the model. Force transducers located under each bearing measured shear, axial, and bending moment forces. The model was designed to include detachable bracing. The main purpose of the bracing was to ensure that no damage occurred during the design-level tests with the different isolation systems. This permitted direct comparisons between the three systems. The model was not braced in the ultimate-level tests.

Design-Level Earthquake Tests

The design-level earthquake test program investigated the performance of the isolated braced model when subjected to ground motions with intensities specified by the Japanese seismic code. Initially, dynamic characteristics of the model were determined using low-amplitude forced-vibration tests, dynamic pull-back tests, and white-noise input tests. The first and second frequencies of the braced fixed-base model were determined to be approximately 6.8 Hz and 19.6 Hz, respectively. Three earthquake motions were applied to the model on each of the isolation systems. The earthquakes used were the 1940 El Centro (N-S), 1968 Hachinohe (N-S), and 1978 Miyagi (N-S) records. Each of these motions was input at two intensities, corresponding to peak velocities of 10 in./sec. (25 cm/s) and 20 in./sec. (50 cm/s) for the prototype structure. These velocities are the two design levels specified by the Japanese seismic design code for conventional buildings.

The response of the model isolated on each of the three systems in turn when subjected to the three test motions is summarized in Table 1. The input level is indicated as design-level 1 (10 in./sec. full scale) or design-level 2 (20 in./sec. full scale) in the table. Model story shear maxima for each of the three isolation systems subjected to the design-level 1 motions are shown in Figure 5, and for the design-level 2 motions in Figure 6.

The design-level 2 Miyagi motion was the most severe input for the high-damping A and lead-rubber systems, while the design-level 2 Hachinohe motion was most severe for the high-damping B system. The high-damping B system proved to be the most effective of the three designs in terms of reducing the accelerations, story drifts, and shears induced in the superstructure. For the El Centro and Miyagi motions, the high-damping B system reduced the roof acceleration to about 40 percent of the input level. For the worst-case Hachinohe design-level 2 motion, the high-damping B system reduced the roof acceleration to about 50 percent of the input level. The high-damping B system limited the peak base shear ratio to 0.18 or less for all inputs, while for the other two bearing systems this value was 0.23 for design-level 1 and 0.41 for design-level 2. The high-damping A and lead-rubber systems both caused very small amplifications of acceleration (only about one percent) at the roof level for their worst-case inputs (Table 1). The reason for the greater superstructure acceleration and force reductions with the high-damping B system is the lower shear stiffness and thus longer period of that system compared to the other two systems. The equivalent prototype period of the high-damping B system was approximately 2.0 seconds and 2.8 seconds, for the design-level 1 and design-level 2 motions, respectively. The nonlinearity of the rubber compound and the hysteresis behavior of the bearings is the cause of the input amplitude- or intensity-dependent period. The high-damping A and lead-rubber systems had shorter predominant periods — both about 1.2 seconds and 1.5 seconds for the design-level 1 and 2 motions, respectively. The relatively longer period of the high-damping B system resulted in lower spectral accelerations, but with correspondingly larger spectral displacements. This effect

is seen in the response quantities in Table 1, where the maximum bearing displacements of the high-damping B system are significantly larger than those of the other two systems.

The model was also subjected to two actual earthquake ground motions that were recorded at the site of the full-size building in Sendai. The response of the model was compared with the recorded response of the full-size building. Agreement was reasonable, but the intensities of shaking were very small (about 0.02g), and the results are not discussed in any further detail here.

Ultimate-Level Earthquake Tests

At the conclusion of the tests of the braced model, the bracing was removed and two large-input tests were performed with the model on the design 1 high-damping A bearings. The two tests were Miyagi, with a PGA of 0.77g, and the SCT station recording of the 1985 Michoacan earthquake, with a PGA of 0.48g. The corresponding full-scale peak velocities for these two inputs were 24.1 in./sec. and 23.9 in./sec., respectively. The SCT motion is particularly severe for isolation systems because it has a very well-defined spectral peak at 2 seconds, almost exactly at the design period for many isolation systems. In the case of the model on the high-damping A system, the SCT motion represented essentially a resonance excitation. Even so, it was possible to subject the isolated model to the SCT signal at 2.3 times the actual recorded intensity. The response of the model in the two large-input tests is summarized in Table 2. In both tests the isolation bearings deformed sufficiently to reach the high-strain stiffening range — 286 percent strain in the Miyagi test and 321 percent strain in the SCT test. The hysteresis loop for the complete isolation system for the SCT test is shown in Figure 7. Stiffening of the bearings ensured that in both tests substantial shear forces entered the superstructure. The peak base shear ratios (V_b/W) were 0.73 and 0.67 in the Miyagi and SCT tests, respectively. These force levels are approximately the lateral capacity of the building, determined by static collapse analysis, and confirmed by the extensive inelastic action recorded by the rebar strain gauges throughout the superstructure. Figure 9 shows the extent of yielding in the model.

The maximum deformation of the bearings in the SCT test, 321 percent, while inducing substantial forces in the superstructure, did not come close to the shear capacity of the bearings. The failure strain of 739 percent shown in Figure 8 implies a factor of safety (in terms of displacement) of the bearings of 2.3.The equivalent shear force safety factor is 6.2. These bearing safety factors, at the lateral capacity of the superstructure, indicate that the bearings have substantial margins beyond the maximum loading conditions.

Isolated and Fixed-Base Comparison Tests

The original fundamental frequency of the unbraced fixed-base model was 4.5 Hz. System identification analyses after the ultimate-level tests showed that the damage to the model represented about a 66 percent loss of stiffness from its original condition. Epoxy-injection grouting was used to repair as much of the model as possible. The repair recovered a reasonable amount of stiffness, raising the fundamental frequency to 2.9 Hz.

With the repaired model isolated on the high-damping A bearings, the design-level 1 El Centro motion was input. The peak base shear ratio (V_b/W) was 0.14 in this test, and no damage was apparent in the superstructure. After this single test the isolators were removed, and the model was connected directly to the force transducers on the shake table. The design-level 1 El Centro signal was then input to the now fixed-base model. The peak base shear ratio was 0.40 and significant cracking in the joint regions and at the column bases occurred. Strain gauge recordings indicated yielding in a number of locations. The fundamental frequency of the model after this test was 2.3 Hz. The results of these two tests provide a direct experimental comparison of the performance of base-isolated and equivalent fixed-base structures. Roof acceleration

time-histories from the two tests are compared in Figure 10. The longer-period and reduced-amplitude response of the isolated model is clearly seen. In the fixed-base model the peak roof acceleration was 0.72g, while in the isolated model the peak was only 0.25g. Peak interstory drift ratios were 1.0 percent in the fixed-base model and 0.39 percent in the isolated model. Comparisons of peak drift ratio, story acceleration, and story shear are shown in Figure 11.

Conclusions

This study contained a number of significant achievements. It was the first earthquake simulator study of a model of an actual base-isolated building, and the first study of a code-compliant isolated concrete building. In this regard, the results represent an extremely useful dataset for evaluating and confirming current design practices.

Three types of elastomeric isolation bearings were evaluated, in terms of both the mechanical characteristics of individual bearings, and the seismic response of a three-story concrete model isolated with each type of bearings. The bearing component tests permitted a detailed investigation of mechanical properties, and the results will be used to calibrate analytical models of isolation bearings.

The model was subjected to a series of design-level earthquake tests, which was repeated for each of the three bearing systems. The longer isolated period of the high-damping B system proved to be the most effective of the three systems in terms of floor acceleration and story shear response reductions. At the same time, however, this "softer" system had to sustain larger displacements than the other two systems. The small response differences between the high-damping A and lead-rubber systems, which were designed to have the same stiffness characteristics, were a result of the higher damping of the lead-rubber system.

The ultimate-level tests demonstrated that the isolated model was capable of withstanding very severe earthquake inputs. The lateral capacity of the model was reached in these tests, and even then, the isolation bearings still had a displacement safety margin of about 2.3 and a shear force safety margin of 6.2. Tests of the model in isolated and fixed-base configurations provided experimental data for direct comparisons between otherwise equivalent structures subjected to the same El Centro motion. The results show the substantial benefits of seismic isolation.

Detailed studies and nonlinear correlative analyses of the design-level and ultimate-level shake table tests are ongoing and will contribute significantly to the general knowledge and understanding of the behavior of isolated structures under extreme levels of earthquake shaking.

References

Aiken, I.D., Kelly, J.M., Clark, P.W., Tamura, K., Kikuchi, M., and Itoh, T., 1992, "Experimental Studies of the Mechanical Characteristics of Three Types of Seismic Isolation Bearings," *Proceedings, 10th World Conference on Earthquake Engineering*, Vol. 4: 2281-2286, Madrid, Spain, July.

Izumi, M., Tobita, J., Kurosawa, I., Miyazawa, F., and Kubota, K., 1990, "Earthquake Response Characteristics of Base-Isolated Buildings by Direct Comparison with a Non-Isolated One," Architectural Reports of the Tohoku University, No. 29, Sendai, Japan.

Saruta, M., Watanabe, H., and Izumi, M., 1989, "Proof Test of Base-Isolated Building Using High Damping Rubber Bearing," *Transactions, 10th International Conference on Structural Mechanics in Reactor Technology*, Vol. K: 631-636, Los Angeles, August.

Yamahara, Y., and Izumi, M., 1987, "Actual Proof Tests of the Base-Isolated Building Using Full-Sized Model," Shimizu Corporation and Tohoku University, Japan.

Table 1. Summary of Braced Model Responses, Design-Levels 1 and 2 Tests

	ISOLATION SYSTEM	Design Level	PGA [g]	γ_{max} [%]	Bearing Displ. [in.]	$\left[\frac{V_b}{W}\right]_{max}$	Roof Drift [%]	$\left[\frac{\text{Roof Accn.}}{\text{PGA}}\right]_{max}$
EL CENTRO	High-Damping A	1	0.32	60	1.04	0.18	0.10	0.60
		2	0.51	109	1.89	0.27	0.13	0.57
	High-Damping B	1	0.33	125	2.37	0.11	0.07	0.40
		2	0.48	237	4.48	0.18	0.16	0.44
	Lead-Rubber	1	0.31	30	0.75	0.15	0.09	0.55
		2	0.51	63	1.56	0.25	0.15	0.58
HACHINOHE	High-Damping A	1	0.21	56	0.96	0.18	0.09	0.92
		2	0.44	123	2.13	0.28	0.14	0.69
	High-Damping B	1	0.20	157	2.96	0.13	0.11	0.76
		2	0.42	263	4.96	0.17	0.20	0.48
	Lead-Rubber	1	0.21	34	0.85	0.16	0.09	0.81
		2	0.42	71	1.77	0.27	0.18	0.72
MIYAGI	High-Damping A	1	0.34	93	1.62	0.23	0.15	0.80
		2	0.46	195	3.37	0.41	0.18	1.01
	High-Damping B	1	0.23	79	1.50	0.07	0.07	0.39
		2	0.46	163	3.09	0.13	0.13	0.33
	Lead-Rubber	1	0.25	51	1.25	0.22	0.14	1.01
		2	0.47	118	2.93	0.37	0.27	0.96

Table 2. Summary of Unbraced Model Responses, Ultimate-Level Tests

EARTHQUAKE SIGNAL	PGA [g]	γ_{max} [%]	Bearing Displ. [in.]	$\left[\frac{V_b}{W}\right]_{max}$	Peak Drift [%]	$\left[\frac{\text{Roof Accn.}}{\text{PGA}}\right]_{max}$
Miyagi	0.77	286	4.96	0.73	1.46	1.05
SCT	0.48	321	5.56	0.67	1.62	1.72

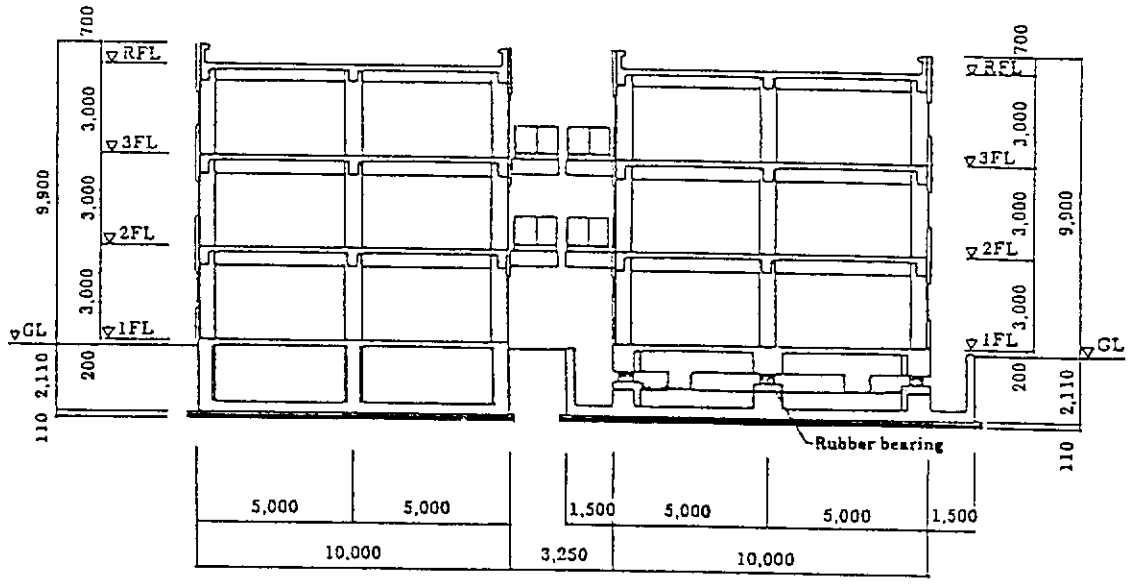

Figure 1. Elevation of Tohoku University Test Buildings

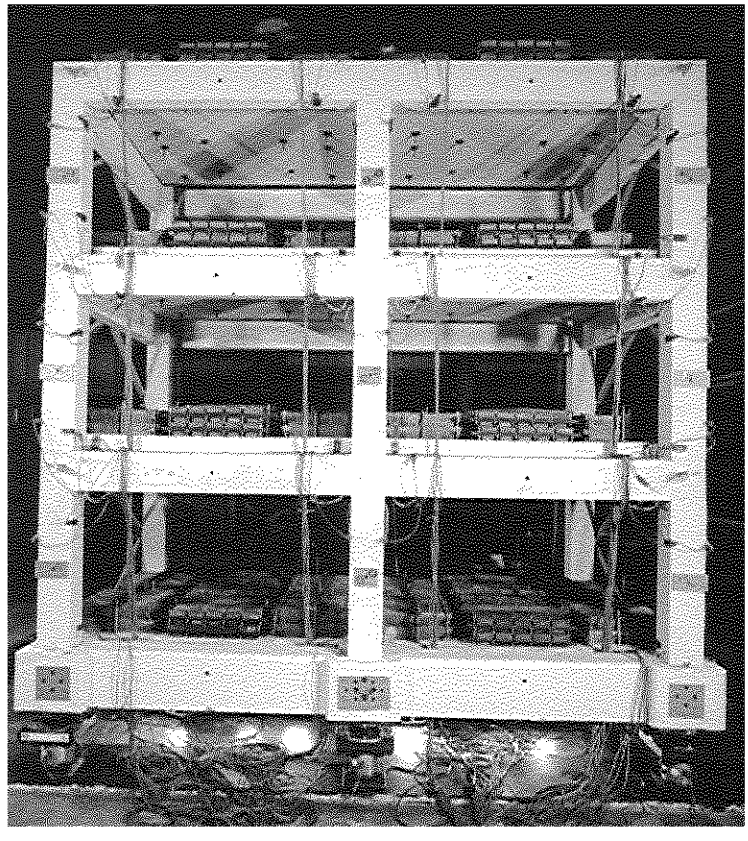

Figure 2. 1/2.5-Scale Model of Isolated Building on Shake Table

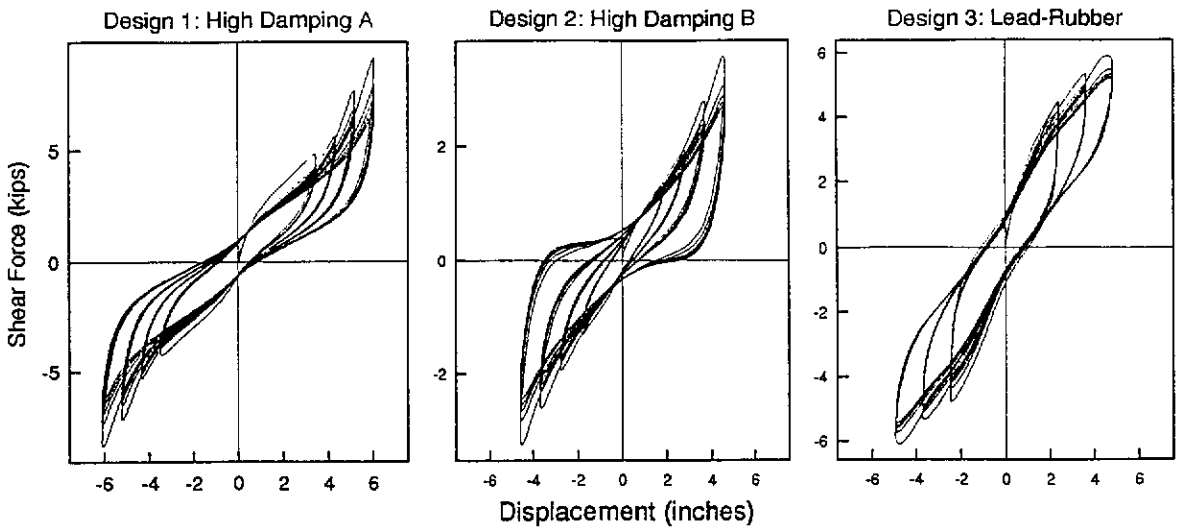

Figure 3. Bearing Shear-Force Displacement Hysteresis Loops

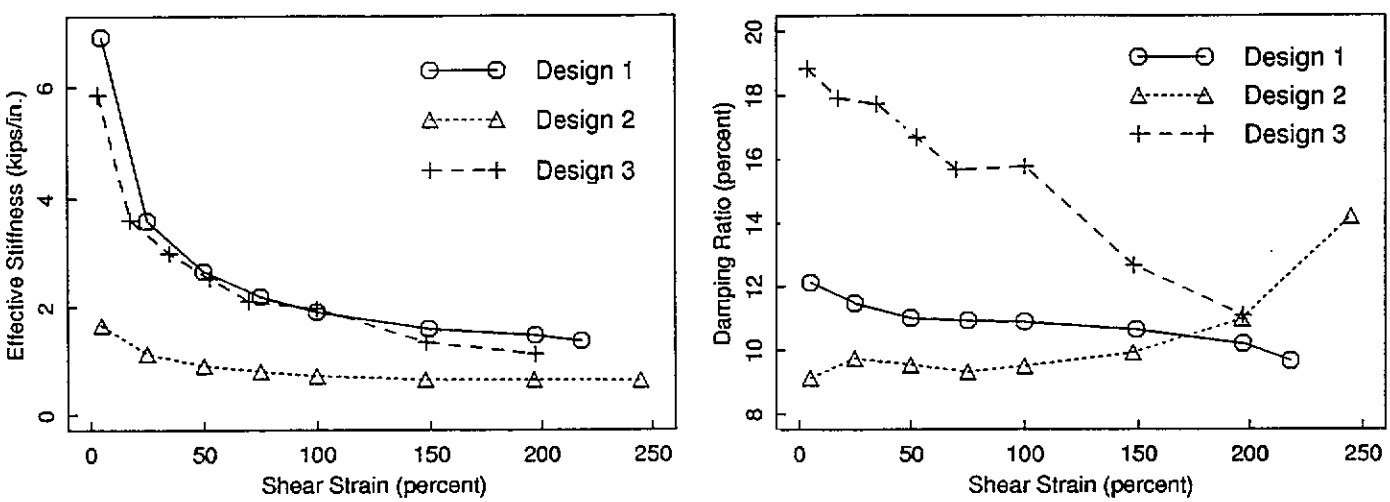

Figure 4. Bearing Stiffness and Damping, All Three Designs

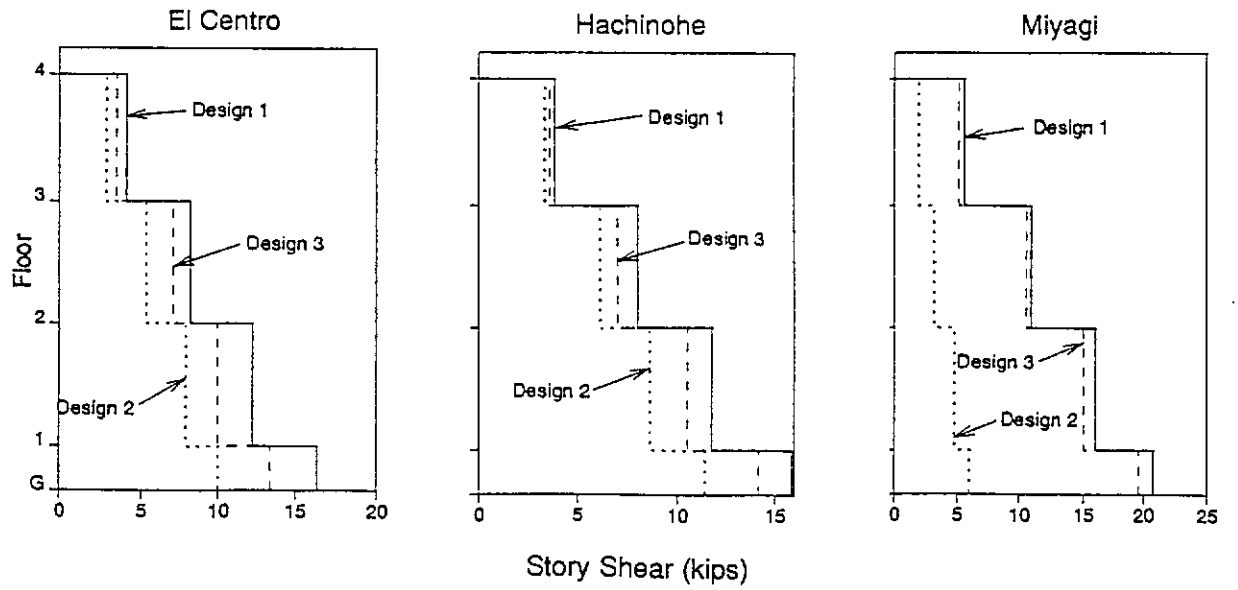

Figure 5. Peak Story Shears in Braced Model, Design-Level 1 Tests

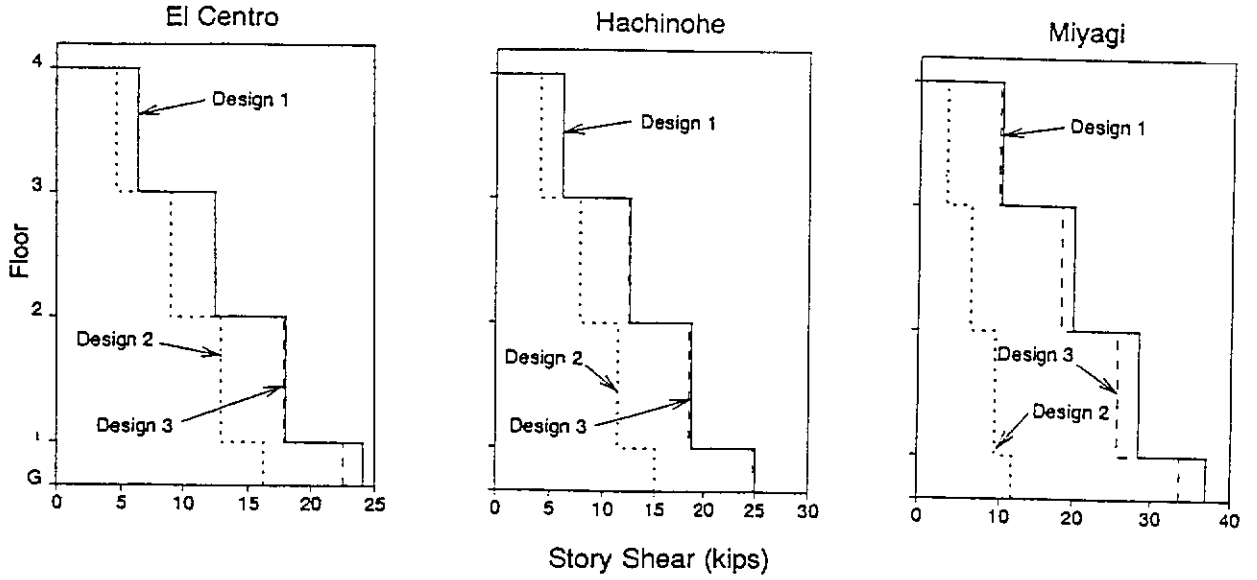

Figure 6. Peak Story Shears in Braced Model, Design-Level 2 Tests

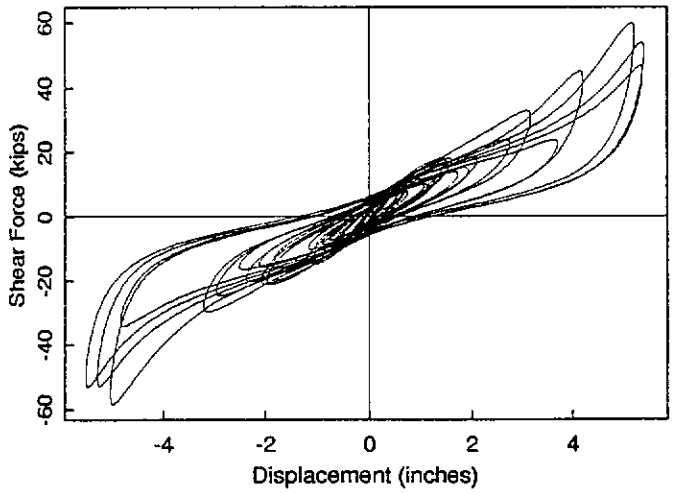

Figure 7. Complete Isolation System Hysteresis for SCT Ultimate-Level Test

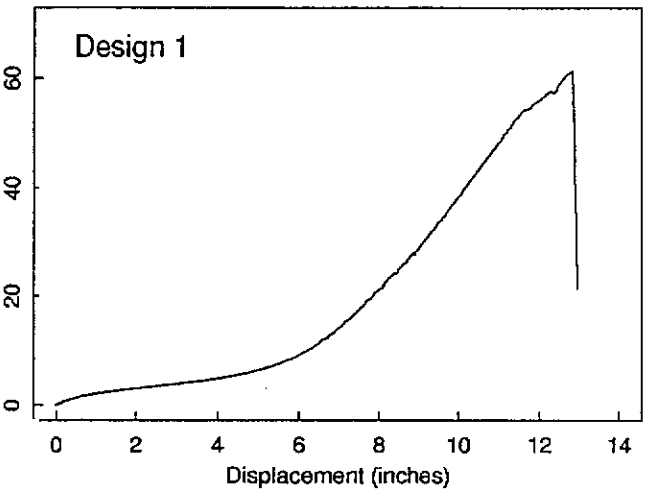

Figure 8. Monotonic Shear Failure, One Bearing

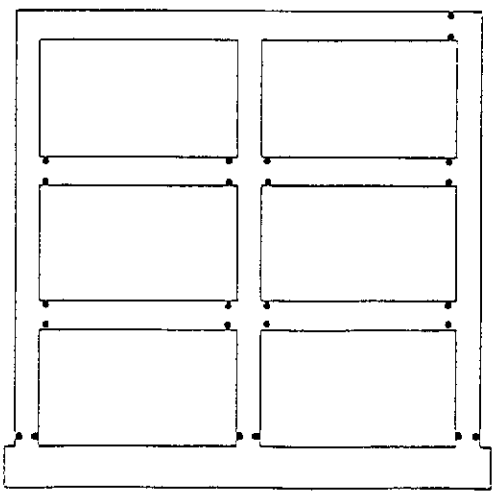

• Yielding Locations

Figure 9. Locations of Yielding in Model for SCT Ultimate-Level Test

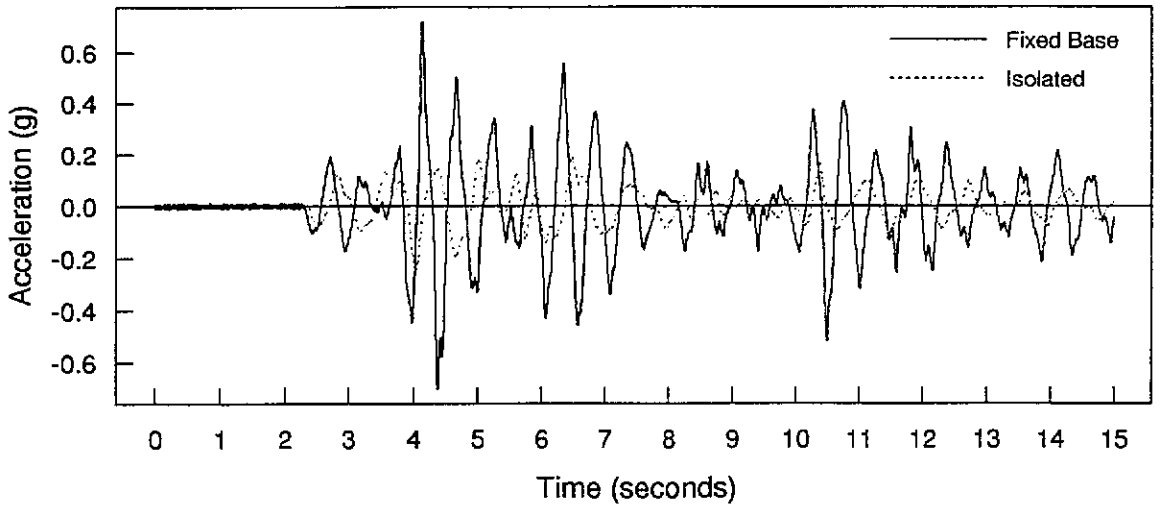

Figure 10. Isolated vs. Fixed-Base Roof Accelerations, El Centro Design-Level 1 Test

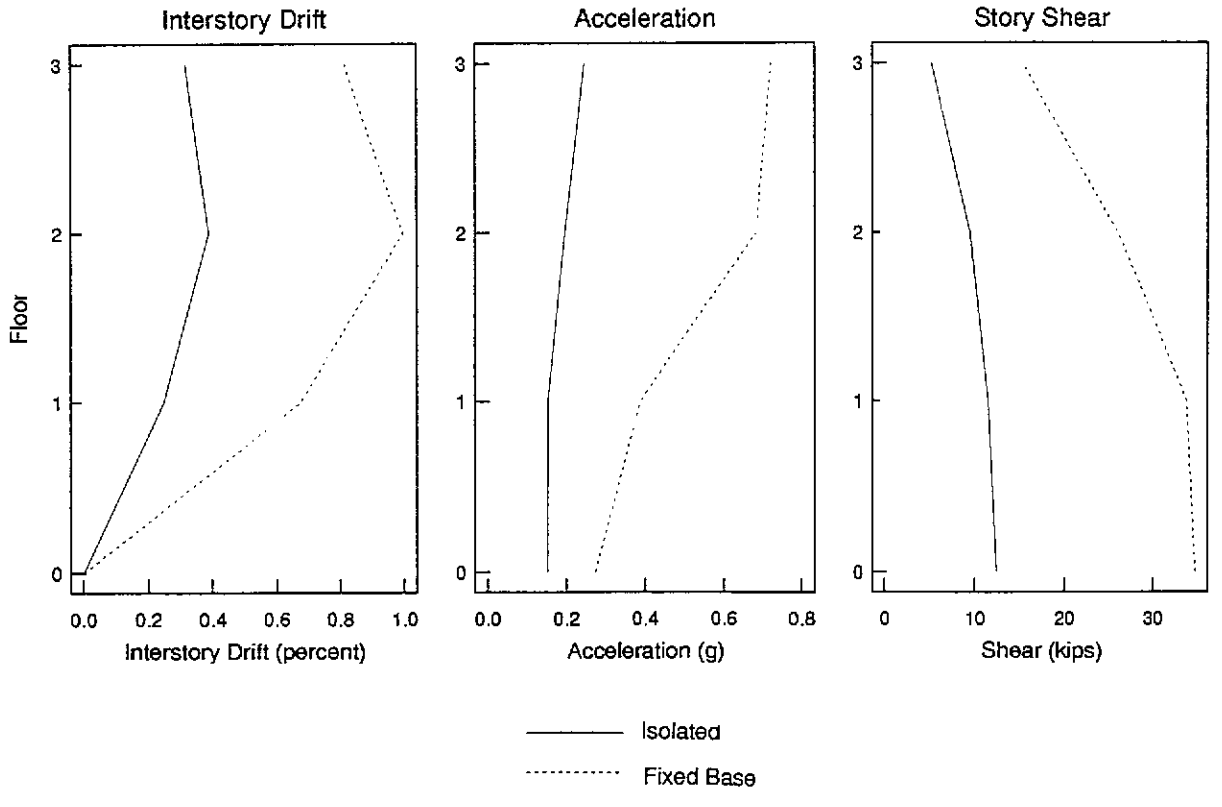

Figure 11. Isolated and Fixed-Base Responses, El Centro Design-Level 1 Test